

$$\frac{\partial(\rho k)}{\partial t} + \nabla \cdot (\rho V k) = \nabla \cdot \left(\left(\mu + \frac{\mu_t}{\sigma_k} \right) \nabla k \right) + G_k - \rho \varepsilon \quad (6)$$

$$\frac{\partial(\rho \varepsilon)}{\partial t} + \nabla \cdot (\rho V \varepsilon) = \nabla \cdot \left(\left(\mu + \frac{\mu_t}{\sigma_\varepsilon} \right) \nabla \varepsilon \right) + C_1 \frac{\varepsilon G_k}{k} + C_2 \rho \frac{\varepsilon^2}{k} \quad (7)$$

where G_k is the generation of turbulence kinetic energy due to mean velocity gradients; C_1 and C_2 are constants; σ_k and σ_ε are respectively turbulent Prandtl numbers for k , and ε ; μ_t is turbulent viscosity expressed as:

$$\mu_t = C_\mu \rho k^2 / \varepsilon \quad (8)$$

With a mean rate of strain tensor $S_{i,j}$ taken into account, the renormalization group (RNG) k-epsilon model was finally chosen as it is more responsive to the effects of rapid strain and streamline curvature than the standard k-epsilon model^[5]. And the values of the equation coefficients^[6] are

$$\left. \begin{aligned} C_\mu &= 0.0845; C_1 = 1.42 - \frac{\tilde{\eta}(1 - \tilde{\eta}/\tilde{\eta}_0)}{1 + \beta\tilde{\eta}^3}; C_2 = 1.68 \\ \sigma_k &= 0.7179; \sigma_\varepsilon = 0.7179; \tilde{\eta} = Sk / \varepsilon \\ S &= (2S_{i,j}S_{i,j})^{1/2}; \tilde{\eta}_0 = 4.38; \beta = 0.015 \\ S_{i,j} &= \frac{1}{2} \left(\frac{\partial u_i}{\partial x_j} + \frac{\partial u_j}{\partial x_i} \right) \end{aligned} \right\}$$

2.2. Aerodynamic model

Dynamic mesh CFD for a propeller aircraft can become very expensive in terms of CPU time. Consider the three-dimensional models of E-2C aircraft, as shown in Fig.1. The diameter of the propeller is 4.14m, around which millions of mesh will be smoothed and computed in each time step.

MRF model, however, introduces a rotate velocity to the frame of rotating fluid zone around the aircraft propeller without mesh recomputation. This reduces the run time dramatically. The inlet, outlet, and wall boundary conditions are designed 15 times the length of the aircraft away from the aircraft to get a solution that is independent of the their exact position, and a symmetry of the model has been adopted.

Aircraft outside surface and the deck ground are set as adiabatic wall. Details about the model is illustrated in Fig.2. Two parts of fluid zone are meshed with unstructured mesh respectively and then assembled together. Interfaces are defined for the interpolation of fluxes and conserved variables from one side to the other. Fluid environment temperature is 300K with standard atmospheric pressure. T56-A-427 Engine made by Allison Engine Company is adopted by E-2C, the air mass flux of the engine is about 15.2kg/s^[1], and the temperature of the exhaust gas is set as 750K. Rotate speed of the propeller is set as 1000rpm.

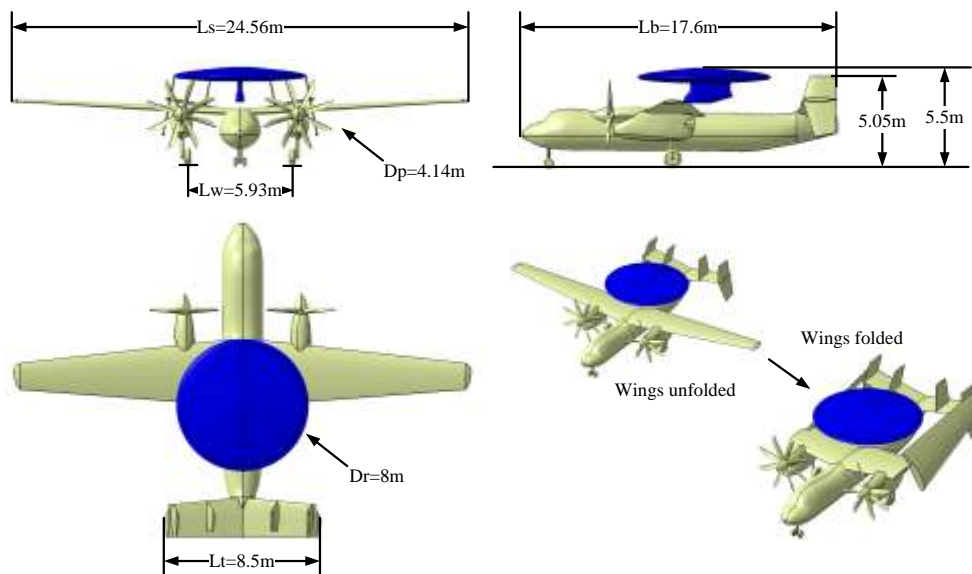


Fig.1 The three dimensional model of E-2C

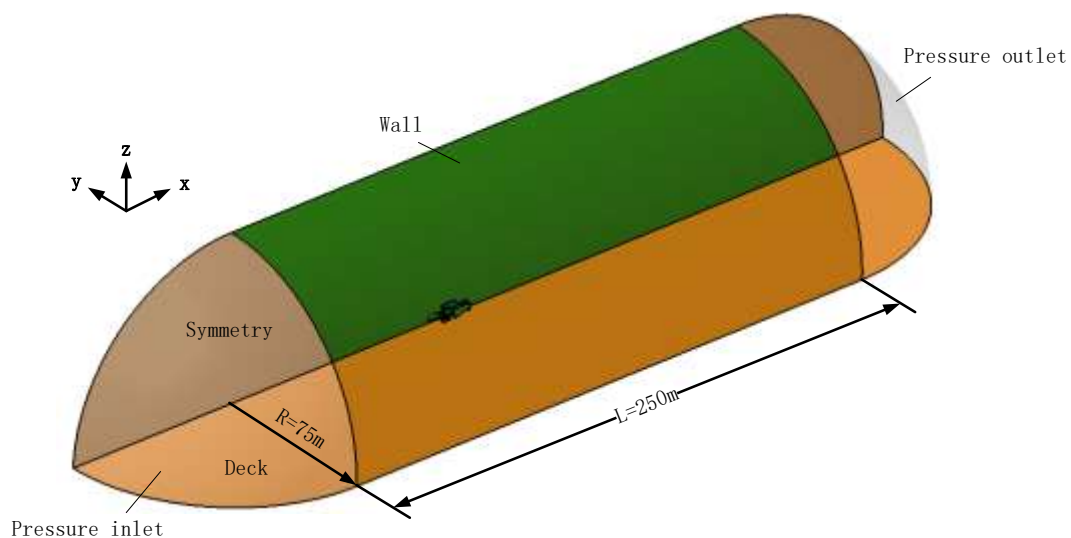


Fig.2 The aerodynamic model

2.3. Structural model

According to the CFD results, the outer vertical tail was found to be the seriously heated area and further structural thermal analysis was required. Therefore, a structure model of the vertical tail has been supplied, as shown in Fig.3. This model contained details about the lower vertical stabilizer including the leading edge, axle beams, ribs, outer skins and stiffeners, besides, the rudders and the rest of structures which remained normal temperature were simplified as solid part. Structures were primarily made by metal, here TC4 titanium alloy was chosen. However, the leading edges of the empennage were designed to be made by fiber reinforced composite materials for reducing the vertical tail resistance effect on the radar performance. The material parameters are shown in Tab.1.

ABAQUS 6.14-1 was utilized to analyze the heat transfer process through the vertical tail and the thermal strain of each component. Structures were tied together on contact surfaces, and a total of 62 tie constraints have been created. The initial temperature of the vertical tail was pre-defined as 300K. Solid elements, C3D8T, with both thermally coupling and trilinear capabilities, were used to discretize the whole structure model. The stacking sequence of the leading edge composite layers was defined as [-45°/0°/45°/90°].

Tab.1 Material parameters

	E_1/GPa	E_2/GPa	E_3/GPa	G_{12}/GPa	G_{13}/GPa	G_{23}/GPa	μ_{12}	
CCF300	142	9.46	9.46	5.6	5.6	3.8	0.25	
/5228A	μ_{13}	μ_{23}	$\rho/\text{g}\cdot\text{cm}^{-3}$	$\lambda/\text{W}\cdot\text{K}^{-1}$	$C_p/\text{J}\cdot(\text{kg}\cdot\text{K})^{-1}$	α_1/K^{-1}	α_2/K^{-1}	α_3/K^{-1}
	0.25	0.4	1.7	500	800	1.5e^{-5}	3.54e^{-5}	3.54e^{-5}
	E/GPa	μ	$\rho/\text{g}\cdot\text{cm}^{-3}$	$\lambda/\text{W}\cdot\text{K}^{-1}$	$C_p/\text{J}\cdot(\text{kg}\cdot\text{K})^{-1}$	α/K^{-1}		
TC4	108	0.3	4.44	7200	615	9.1e^{-6}		

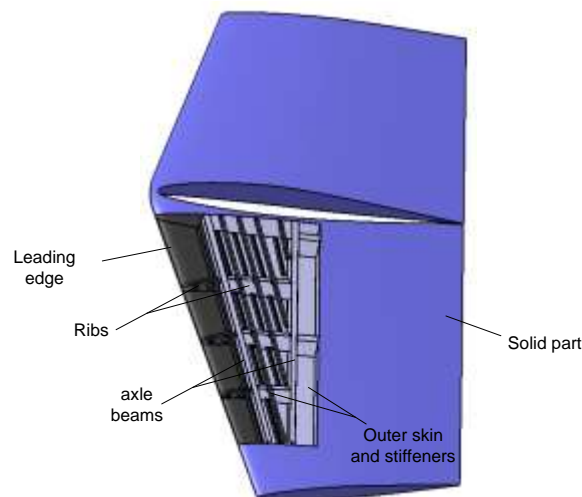


Fig.3 Outer vertical tail structure model

2.4. Fluid-thermal-structure coupling method

In general, there are two different approaches of code coupling^[7]. Monolithic coupling approach solved both disciplines in one system of equations, without any interpolation at the interface of flow and structure but required identical discretizations for both domains. Partitioned code coupling however employs separate discretizations for each discipline but requires interpolation at the interface. Within this work, the CFD solver of FLUENT 15.0 is unidirectionally coupled to the CSD solver of ABAQUS 6.14.1 via MpCCI 4.4.1, as shown in Fig.4.

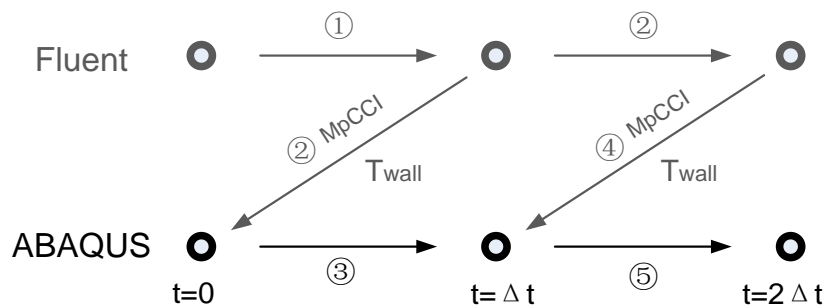


Fig.4 Unidirectional partitioned coupling approaches

3. RESULTS

3.1. CFD Results and discussion

For prediction of seriously heated area locations on E-2C aircraft, steady thermal flow field computations with wings unfolded and folded were both performed. The CFD mesh was comprised of about 5200,000 tetrahedral cells computed using ICEM CFD. The flow was treated as compressible ideal gas.

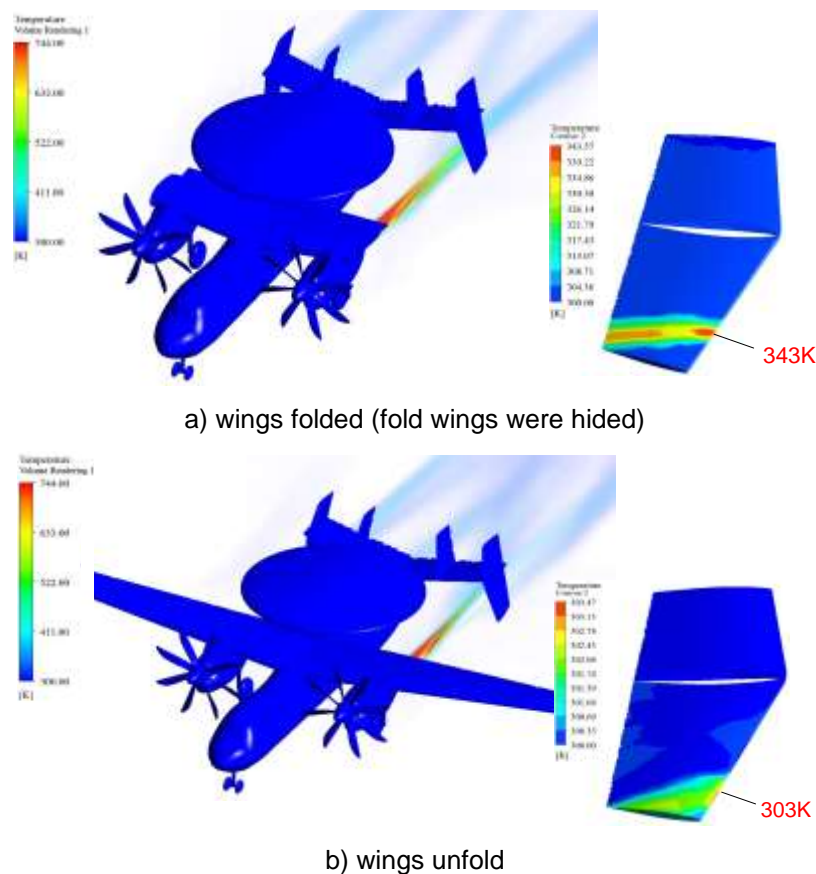


Fig.5 Temperature contours of E-2C aircraft

Full Multigrid initialization (FMG initialization) was used at the start of calculation as it could provide a better initial solution and flow convergence for rotating machinery

condition^[5]. The CFD results showed a seriously heated area location at the lower vertical tail, especially at the composite leading edge when wings were folded, as seen in Fig.5, the max temperature was about 70 degrees centigrade while the vertical tail remained a normal temperature of 30 degrees centigrade with wings unfolded. It could be found that an obvious heat up would occur on the vertical tail when wings had been folded. Besides, the thermal flows showed little affects on structures in other places of the aircraft where the temperature was below 33 degrees centigrade.

Deflections have been found in the wake of exhaust flow due to the Bernoulli Principle that an increase in the speed of a fluid occurred simultaneously with a decrease in pressure, as shown in Fig.6. When wings were unfolded, the propeller race under the outer wing panel spread over a wide range of areas while it was limited in a narrow space between the engine and the fuselage on the other side. The flow which was closed to the fuselage gained a higher velocity. And a flow deflection away from the vertical tail appeared, making for little thermal effect on the structures. However, as the wings were folded, the situation changed and propeller race around the fold wings became a bit faster than the other side around the fuselage. Exhaust flow from the engine tail pipes, in this case, deflected away from the fuselage to the vertical tail, heating up structures. As a result, exhaust flow and propeller race interacted with each other, formed a high temperature flow with a clockwise rotation which is the same as the rotating direction of the propeller.

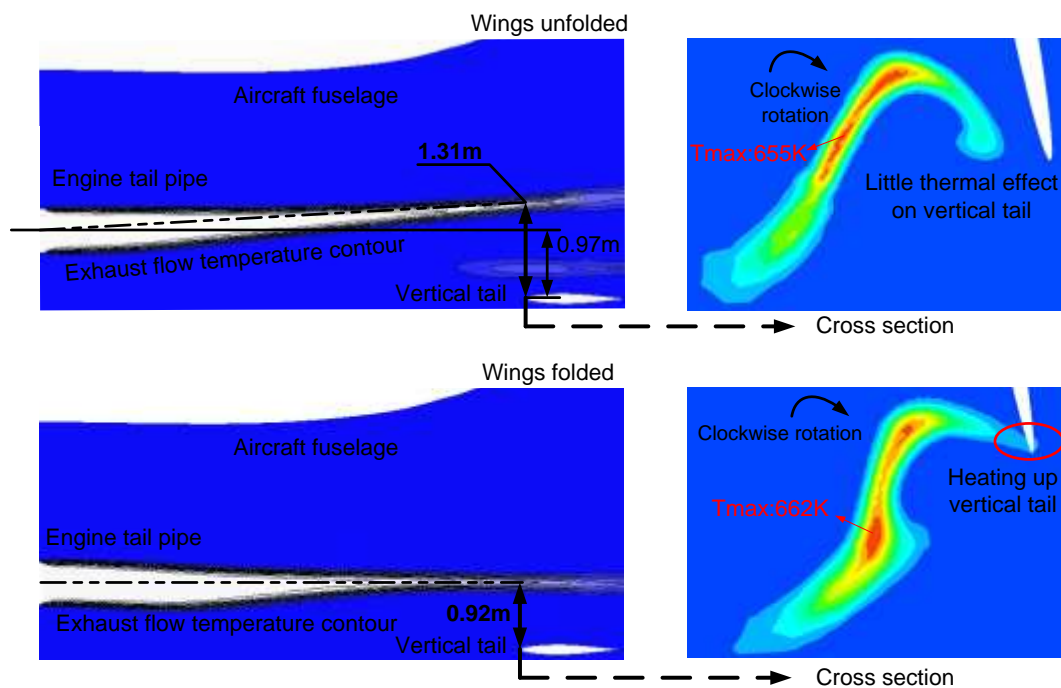


Fig.6 Temperature contour cross-sectional views of the thermal flow

3.2. CSD Results and discussion

A maximum temperature of about 70 degrees centigrade was found to appear at the leading edge of the outer vertical tail which required further structural thermal analysis. MpCCI was used to transfer the wall temperature unidirectionally from CFD

results to the FE-code as boundary conditions of heat transfer analysis, as shown in Fig.7. Regardless of the complex heat convection between the structure and the fluid, here a more conservative result has been obtained.

A steady coupled temperature-displacement analysis was presented using the temperature data in the steady CFD results. Time period was set as 10 with a fixed increment of 0.1. The CSD results showed that the maximum principal strain in the vertical tails appears at the boundary of the composite leading edge, as seen in Fig.8, the value is about 1700 microstrains, while in other metal structures the maximum principal strain was only 784 microstrains. Periodic thermal strain on the leading edge which was made by composite materials would result in thermal fatigue and adversely affected the mechanical performance, besides, structures became apt to undergo chemical corrosion in the wet environment on sea. A structure enhancement or some special thermal protection such as Thermal barrier coatings (TBCs) was suggested.

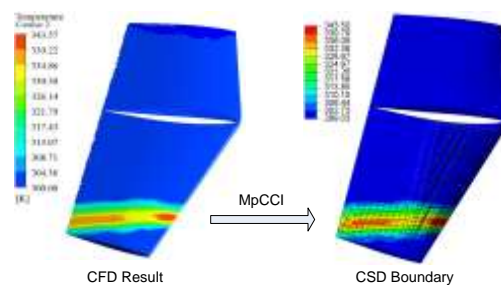


Fig.7 Wall temperature unidirectional coupling through MpCCI

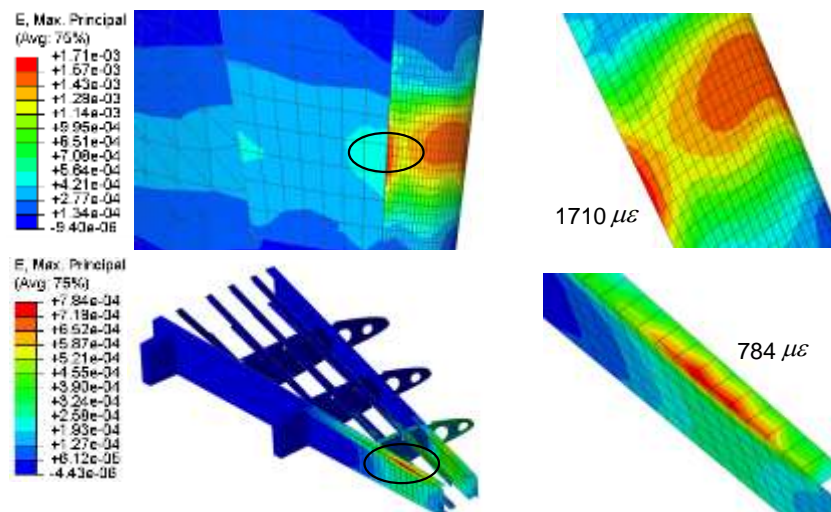


Fig.8 Thermal strain results of vertical tail

4 CONCLUSIONS

This paper describes the demonstration of a unidirectionally coupled fluid-thermal-structure procedure using ABAQUS and Fluent to analyze the thermal effect of engine exhaust jet flow on the structures of E-2C carrier-based airborne early-warning aircraft. When wings are folded, the vertical tail is found to be the most seriously heated area, the maximum temperature value is 70 degrees centigrade. The maximum thermal strain in the vertical tails appears at the boundary of leading edge with a value of 1710

microstrains, which suggests some special treatment for structure enhancement and thermal protection. The results demonstrate that the ABAQUS/MpCCI/Fluent coupling method is capable of analyzing the thermal fluid of E-2C aircraft and its effects on aircraft structures.

REFERENCES

- [1] Li Shouze, Luo Yansheng. E-2 Hawkeye airborne early warning aircraft [M]. Beijing: Aviation Industrial Publishing House, 2013:14-15.
- [2] Obaid Younossi, Mark V. Arena, Michael Boito, Jim Dryden, Jerry Sollinger. The Eyes of the Fleet: A Analysis of the E-2C Aircraft Acquisition Options[M] . Santa Monica: RAND, 2002.1-84.
- [3] Sanjay R. Mathur. Unsteady Flow Simulations Using Unstructured Sliding Meshes[C]. 1994, 25th AIAA Fluid Dynamics Conference, Colorado Springs, CO. AIAA, Washington, D.C., USA.
- [4] A. Filippone. Simulation of Rotating Cylinder with Sliding Meshes[C]. 2005, 43rd AIAA Aerospace Sciences Meeting and Exhibit. Reno, Nevada, USA.
- [5] ANSYS, Inc. Southpointe, 2013. ANSYS Fluent Theory Guide. Release 15.0. <http://148.204.81.206/Ansys/150/ANSYS%20Fluent%20Theory%20Guide.pdf>.
- [6] Speziale C G, Thangam S. Analysis of an RNG based turbulence model for separated flows. Int J Engng Sci. 1992. 10:1379-1388.
- [7] Sven Schrape, Jens Nipkau, Arnold Kühhorn, Bernd Beirow. Application of aeroelastic methods in compressor cascade configurations using commercial code coupling. 2008 ASME Pressure Vessels and Piping Division Conference. Chicago, Illinois, USA.
- [8] Gu Rui, Xu Jinglei, Mo Jianwei, Yu Yang. Primary analysis of fluid-structure interaction of adjustable SERN on the different cowl position. 2012, 18th AIAA/3AF International Space Planes and Hypersonic Systems and Technologies Conference. Tours, France.